

# Phonon-Polaritons in Nanoscale Waveguides

Hashem Zoubi\*

*Department of Physics, Holon Institute of Technology, Holon 5810201, Israel*

(Dated: 09 April, 2018)

We investigate the phenomena of Brillouin induced opacity in nanoscale linear waveguides and Brillouin induced transparency in nanoscale ring waveguides. The concept of phonon-polariton is required in order to get a deep understanding of such phenomena. Phonon-polaritons are coherent superposition of photons and phonons obtained in the strong coupling regime induced through stimulated Brillouin scattering in the presence of a pump field. The formation of phonon-polaritons can be observed via linear optical spectra that are calculated here using the input-output formalism. For a linear waveguide the signature of phonon-polaritons appears as two peaks in the transmission spectrum with an opacity gap, and for a ring waveguide as two dips in the transmission spectrum with a transparency gap.

## I. INTRODUCTION

Stimulated Brillouin Scattering (SBS), or the scattering of light from mechanical excitations of a medium [1, 2], was reported by Brillouin in (1922) but observed till after the invention of the laser by Chiao et al. in (1964) [3]. In the recent years big progress took place in fabricating waveguides with nanoscale cross section that opens new horizons for SBS. A breakthrough has been appeared for SBS in which radiation pressure dominates over the conventional electrostriction mechanism, as predicted in [4] theoretically and realized later experimentally [5]. Radiation pressure can provide strong photon-phonon interactions that lead to a significant enhancement of SBS in nanoscale waveguides at relatively low power [6]. Such a progress introduces SBS as a promising candidate for quantum information processing involving photons and phonons [7–12].

Several proposals appear in the literature for the realization of nanoscale waveguides [13]. Among the main factors that strongly limit the efficiency of each device is the waveguide mechanical quality factor. For example, in on-chip waveguides the quality factor is low, due to a direct contact between the waveguide and the substrate material, and that lead to a relatively fast leak of the phonons into the substrate [14]. On the other hand, suspended nanoscale waveguides, e.g. of silicon nanowires, have higher quality factor with longer phonon lifetime, but they are limited to a very short waveguide length that yields weak SBS [15]. A compromise has been suggested by using nanoscale silicon photonic wires that are supported with a tiny pillar, the fact that keeps a reasonable quality factor and allows the achievement of relatively long waveguides with strong SBS [5, 16, 17].

Controlling the propagation of light in an optical medium can be achieved using Electromagnetic Induced Transparency (EIT), which can produce fast and slow light where coherent destructive interference prevents

electronic excitations within an optical medium [18]. In EIT the phase-matching requirement is automatically satisfied by the existence of the atomic component. On the other hand EIT has been demonstrated in cavity optomechanics through the coupling among vibrational modes and photon modes by means of radiation pressure [19]. Here the photons and phonons are in-resonator localized and the phase-matching is also automatically satisfied [20]. SBS has been suggested for the generation of fast and slow light, while the short lifetime of acoustic phonons considered as an obstacle in front of EIT based on SBS. However, in [21] they demonstrate Brillouin scattering induced transparency in exploiting long-lived propagating light and phonons in a silica resonator under the required phase-matching.

In the present paper we investigate Brillouin Induced Opacity (BIO) in linear nanoscale waveguides and Brillouin Induced Transparency (BIT) in ring nanoscale waveguides. The work is motivated by the recently observed significant photon-phonon coupling in silicon nanowires [5]. Phonon coherence lifetimes in silicon nanowires can easily meet the long-lived coherence that is required for BIT and BIO, where photons and phonons obey the phase-matching requirement for both forward and backward SBS. In the strong photon-phonon coupling regime, when the coupling parameter is larger than the photon and phonon damping rates, the picture of independent photons and phonons breaks down and the physical excitations are new quasi-particles that termed phonon-polaritons, which are a coherent superposition of photons and phonons.

We consider two types of dielectric waveguides: (i) A linear waveguide that is supported with two effective mirrors at the two edges. (ii) A ring waveguide that is coupled to an external nanofiber at a fixed point. Photons and phonons can propagate with fixed wavenumbers to the left and the right along the linear waveguide, or clockwise and counter-clockwise in a ring waveguide, hence the momentum-space representation is appropriate in the present context. In applying the input-output formalism, the external-internal field coupling and the leak of photons through the mirrors in linear waveguides,

---

\*Electronic address: hashemz@hit.ac.il

and through the nanofiber in ring waveguides, are included. The method provides optical spectra, e.g. reflection, transmission and absorption parameters, besides the phase shifts of the transmitted and reflected fields relative to the incident ones. The propagating nature of the photons and phonons in waveguides makes the present discussion significantly different from localized interacting ones inside a resonator, as for cavity quantum optomechanics [22]. We investigate the possibility of BIT and BIO in such systems. In the presence of a pump field, we show that an effective coupling between photons and phonons due to SBS inside the waveguide can result in a complete reflection for an external signal field in linear waveguides, and a complete transmission in ring waveguides. Namely, at a frequency where a resonance appears between an external signal field and a cavity photon, a gap opens and the external signal field is reflected or transmitted. The phenomena is deeply explained in terms of phonon-polaritons.

## II. INTERACTING PHOTONS AND PHONONS IN NANOSCALE WAVEGUIDES

We present first photons and phonons in nanoscale waveguides where the results hold for both linear and ring waveguides. We consider a nanoscale waveguide made of high contrast dielectric material of refractive index  $n$ . The electromagnetic field can freely propagate along the waveguide axis with almost continuous wavenumbers, for enough long waveguide, and is strongly confined in the transverse direction with discrete modes. Here we assume a single active mode in the transverse direction. Exploiting translational symmetry, the wavenumber takes the values  $k = \frac{2\pi p}{W}$ , where  $W$  is the waveguide length with ( $p = 0, \pm 1, \pm 2, \dots, \pm \infty$ ). Moreover, we concentrate in a region where light can propagate with almost linear dispersion of an effective group velocity of  $v_g$ . Hence, the photon dispersion is given by  $\omega_k = \omega_0 + v_g k$ , around a given frequency  $\omega_0$  in the appropriate region. The photon dispersion is schematically plotted in figure (1). The photon Hamiltonian in momentum-space representation reads

$$H_{phot} = \sum_k \hbar \omega_k a_k^\dagger a_k, \quad (1)$$

where  $a_k$  and  $a_k^\dagger$  are the creation and annihilation operators of a photon with wavenumber  $k$  for a given transverse mode and a fixed polarization, with frequency  $\omega_k$ .

Next we consider the mechanical vibrations in the waveguide. In nanoscale waveguides different types of vibrational modes can be excited, but here we consider only the propagating acoustic phonons. The acoustic phonons have a linear dispersion that is given by  $\Omega_q = v_a q$ , where  $q$  is the acoustic phonon wavenumber and  $v_a$  is the sound velocity. The phonon dispersion is illustrated in figure (1)

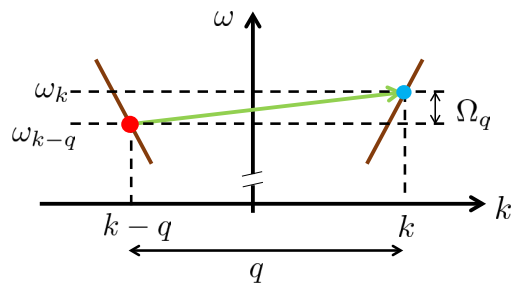


FIG. 1: Schematic plot of the photon dispersion,  $\omega$  vs.  $k$ , for positive and negative wavenumbers. The phonon dispersion,  $\Omega$  vs.  $q$ , is presented. The process of the scattering of a signal photon,  $\omega_k$ , into a pump photon,  $\omega_{k-q}$ , with the emission of a phonon,  $\Omega_q$ , is plotted.

for the acoustic mode. The phonon Hamiltonian reads

$$H_{phon} = \sum_q \hbar \Omega_q b_q^\dagger b_q, \quad (2)$$

where  $b_q$  and  $b_q^\dagger$  are the creation and annihilation operators of a phonon with wavenumber  $q$  for an acoustic mode, of frequencies  $\Omega_q$ .

The SBS among photons and phonons is subjected to conservation of energy and momentum. The SBS Hamiltonian is given by [6]

$$H_{SBS} = \hbar \sum_{kq} \left( g_{kq}^* b_q^\dagger a_{k-q}^\dagger a_k + g_{kq} b_q a_k^\dagger a_{k-q} \right), \quad (3)$$

where  $g_{kq}$  is the SBS coupling parameter among the two photons of wavenumbers  $k$  and  $k - q$  and a phonon of wavenumber  $q$ . The coupling parameter can be in general  $k$  and  $q$  dependent, but we assume here the local field approximation, that is  $g_{kq} = g$ . The first term represents a process in which a photon,  $(k, \omega_k)$ , scatters into another photon,  $(k - q, \omega_{k-q})$ , with the emission of a phonon,  $(q, \Omega_q)$ , under the conservation of energy,  $\omega_k - \omega_{k-q} = \Omega_q$ . The second term represent a photon,  $(k - q, \omega_{k-q})$ , that absorbs a phonon,  $(q, \Omega_q)$ , and scatters into another photon,  $(k, \omega_k)$ , with the conservation of energy,  $\omega_k - \omega_{k-q} = \Omega_q$ . The process is represented schematically in figure (1).

In order to excite the waveguide photons one need to couple the internal field to the external radiation field in using the input-output formalism [23, 24]. We consider first the linear waveguide of a finite length and we assume two effective mirrors at the two edges that are denoted by  $L$  and  $R$ , as seen in figure (2). The mirrors serve us to couple the external field with the internal waveguide field, and also photons can leak outside the waveguide through the mirrors. The input and output external fields of wavenumber  $k$ , from mirror  $L$  are given by  $c_{kL}^{in}$  and  $c_{kL}^{out}$ , and from mirror  $R$  are given by  $c_{kR}^{in}$  and  $c_{kR}^{out}$ , and which are related to the waveguide mode  $k$  by the boundary conditions [23, 24]

$$c_{kL}^{in} + c_{kL}^{out} = \sqrt{u_{kL}} a_k, \quad c_{kR}^{in} + c_{kR}^{out} = \sqrt{u_{kR}} a_k, \quad (4)$$

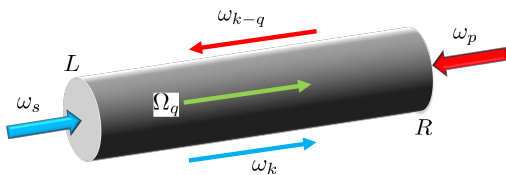


FIG. 2: The linear nanoscale waveguide in which the two sides are considered as two effective mirrors  $L$  and  $R$ , and which allow coupling among external radiation field and internal waveguide field. Inside the waveguide three fields are represented, the photons  $\omega_k$ ,  $\omega_{k-q}$  and the phonon  $\Omega_q$ . Two external fields also appear, the pump field,  $\omega_p$ , on the right, and the signal field,  $\omega_s$ , on the left.

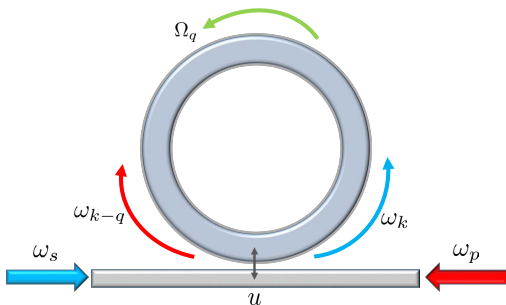


FIG. 3: The ring nanoscale waveguide that is coupled to an external nanofiber with coupling parameter  $u$  that allows tunneling of photons in and out of the waveguide. Inside the waveguide three fields are represented, the photons  $\omega_k$ ,  $\omega_{k-q}$  and the phonon  $\Omega_q$ . Two external fields also appear on the two sides of the external nanofiber, the pump field,  $\omega_p$ , and the signal field,  $\omega_s$ .

where  $u_{kL}$  ( $u_{kR}$ ) is the effective coupling parameter between the internal and external fields of wavenumber  $k$  at mirror  $L$  ( $R$ ). In the following we assume identical mirrors and the coupling is independent of the wavenumber where  $u_{kL} = u_{kR} = u$ . For example, in tapered nanofibers made of silica the tapered zones can be considered as effective mirrors [25, 26]. For nanophotonic waveguides, e.g. made of silicon, grating couplers are used to couple the internal-external fields that considered as effective mirrors [27].

Next we treat a ring waveguide. We assume an external nanofiber to be very close to a waveguide at a fixed point, as seen in figure (3). Photons can tunnel between the waveguide and the nanofiber at this point. The input and output external fields of wavenumber  $k$  are given by  $c_k^{in}$  and  $c_k^{out}$ , which are related to waveguide mode  $k$  by the boundary condition [23, 24]

$$c_k^{in} + c_k^{out} = \sqrt{u_k} a_k, \quad (5)$$

where  $u_k$  is the coupling parameter between the internal and external fields of wavenumber  $k$  at the tunneling point that is proportional to the overlap between the waveguide and the nanofiber fields. In the following we

assume the coupling to be independent of the wavenumber where  $u_k = u$ .

We introduce BIT into a system of a ring nanoscale waveguide, and BIO into a system of a linear nanoscale waveguide, where BIT and BIO require three fields inside the waveguide, a signal photon,  $(k, \omega_k)$ , a pump photon,  $(k-q, \omega_{k-q})$ , and an acoustic phonon,  $(q, \Omega_q)$ . Therefore, we limit our discussion to the Hamiltonian

$$H = \hbar\omega_k a_k^\dagger a_k + \hbar\omega_{k-q} a_{k-q}^\dagger a_{k-q} + \hbar\Omega_q b_q^\dagger b_q + \hbar g^* b_q^\dagger a_{k-q}^\dagger a_k + \hbar g b_q a_k^\dagger a_{k-q}. \quad (6)$$

The first step towards treating BIT and BIO, in adapting the concept of phonon-polaritons, is to bring the Hamiltonian into a quadratic form that includes effective coupling between signal photons and phonons that induced by SBS in the presence of the pump field. This procedure can be achieved in assuming the strong pump field to be a classical one, where the obtained effective photon-phonon coupling is found to be related on the pump field intensity.

We apply two external fields, a strong control field,  $(\omega_p, k-q)$ , that is described by  $c_{k-q}^{in}$ , in order to excite the waveguide pump field, and a weak probe field,  $(\omega_s, k)$ , that is described by  $c_k^{in}$ , in order to excite the waveguide signal field. When the external probe field is tuned to resonance with the signal waveguide field, we expect a strong penetration of the probe field into the waveguide. Here SBS can take place within the waveguide due to the presence of the strong pump field. Induced Brillouin scattering from the signal field to the pump field assisted by an acoustic phonon will appear at the required phase-matching. But a coherent superposition between the system eigenstates inside the waveguide lead to a gap that open in the transmission spectrum and cause a complete reflection of the probe field from the linear waveguide mirror, and a complete transmission for the case of a ring waveguide. In the following we study the process in much details for the two cases of linear and ring waveguides.

Let us concentrate now in the pump field at wavenumber  $k-q$ . The input pump field is represented by  $c_{k-q}^{in}$ . The pump field is enough strong in order to neglect any change in it due to SBS. Hence, using the input-output formalism [23], we get the equation of motion for the pump operator

$$\frac{d}{dt} \tilde{a}_{k-q} \approx -i\Delta_{k-q} \tilde{a}_{k-q} + \sqrt{u} \tilde{c}_{k-q}^{in}, \quad (7)$$

where  $\Delta_{k-q} = \omega_{k-q} - \omega_p - i(u + \frac{\gamma}{2})$ , and we defined  $a_{k-q} = \tilde{a}_{k-q} e^{-i\omega_p t}$ , with  $c_{k-q}^{in} = \tilde{c}_{k-q}^{in} e^{-i\omega_p t}$ . The photon direct damping into free space is included phenomenologically through the damping rate  $\gamma$ .

At steady state we have  $\frac{d}{dt} \tilde{a}_{k-q} = 0$ . Then, for the pump field we get

$$a_{k-q} = \frac{\sqrt{u}}{i\Delta_{k-q}} c_{k-q}^{in}. \quad (8)$$

We define  $\hat{n}_{k-q} = a_{k-q}^\dagger a_{k-q}$ , where  $\hat{n}_{k-q} = \frac{u}{|\Delta_{k-q}|^2} \hat{n}_{k-q}^{in}$ , with  $\hat{n}_{k-q}^{in} = c_{k-q}^{in\dagger} c_{k-q}^{in}$ . The average value is  $n_{k-q} = \langle a_{k-q}^\dagger a_{k-q} \rangle$ , then  $n_{k-q} = \frac{u}{|\Delta_{k-q}|^2} n_{k-q}^{in}$ , with  $n_{k-q}^{in} = \langle c_{k-q}^{in\dagger} c_{k-q}^{in} \rangle$ . Note that  $n_{k-q}^{in}$  has a unit of angular frequency.

### III. PHONON-POLARITONS POINT OF VIEW

We start from the above Hamiltonian (6) that includes only the three appropriate waveguide fields. The system can be linearized by assuming a strong classical pump field, where the Hamiltonian casts into a quadratic one. We use the previous results, where the pump field operator, at steady state in using the input-output formalism, is given by equation (8). In the classical limit we get

$$\beta_{k-q} = \frac{\sqrt{u}}{i\Delta_{k-q}} \alpha_{k-q}, \quad (9)$$

where  $\beta_{k-q} = \langle a_{k-q} \rangle$ , and  $\alpha_{k-q} = \langle c_{k-q}^{in} \rangle$ . We achieve the quadratic Hamiltonian

$$H = \hbar\omega_k a_k^\dagger a_k + \hbar\Omega_q b_q^\dagger b_q + \hbar g^* \beta_{k-q}^* b_q^\dagger a_k + \hbar g \beta_{k-q} b_q a_k^\dagger. \quad (10)$$

We move to a rotating frame that oscillates with the pump waveguide frequency  $\omega_{k-q}$ , in applying the transformation  $H \rightarrow U^\dagger H U - A$ , where  $U = e^{-i\omega_{k-q} t} a_k^\dagger a_k$ , and  $A = \hbar\omega_{k-q} a_k^\dagger a_k$ . We get the Hamiltonian

$$H = \hbar\bar{\omega}_k a_k^\dagger a_k + \hbar\Omega_q b_q^\dagger b_q + \hbar f_{k-q}^* b_q^\dagger a_k + \hbar f_{k-q} b_q a_k^\dagger, \quad (11)$$

where  $\bar{\omega}_k = \omega_k - \omega_{k-q}$ , with the effective coupling

$$f_{k-q} = \frac{g\sqrt{u}}{i\Delta_{k-q}} \alpha_{k-q}. \quad (12)$$

Here we consider the strong coupling regime in which the effective coupling  $|f_{k-q}|$  is larger than the photon and phonon damping rates. The Hamiltonian can be diagonalized by introducing the polariton operators

$$A_{kq}^\pm = X_{kq}^\pm b_q + Y_{kq}^\pm a_k, \quad (13)$$

which are coherent superposition of photons and phonons. The coherent mixing amplitudes are

$$X_{kq}^\pm = \pm \sqrt{\frac{D_{kq} \mp \delta_{kq}}{2D_{kq}}}, \quad Y_{kq}^\pm = \frac{f_{k-q}^*}{\sqrt{2D_{kq}(D_{kq} \mp \delta_{kq})}}, \quad (14)$$

where

$$D_{kq} = \sqrt{\delta_{kq}^2 + |f_{k-q}|^2}, \quad \delta_{kq} = \frac{\bar{\omega}_k - \Omega_q}{2}. \quad (15)$$

We have the normalization condition  $|X_{kq}^\pm|^2 + |Y_{kq}^\pm|^2 = 1$ . The polariton Hamiltonian reads

$$H = \sum_\mu \hbar\Omega_{kq}^\mu A_{kq}^{\mu\dagger} A_{kq}^\mu, \quad (16)$$

with the polariton dispersions

$$\Omega_{kq}^\pm = \frac{\bar{\omega}_k + \Omega_q}{2} \pm D_{kq}. \quad (17)$$

We illustrate the polariton modes using typical nanoscale waveguide numbers. We consider a fixed phonon mode of frequency  $\Omega_q = 10$  GHz, and change the scaled signal frequency  $\bar{\omega}_k = \omega_k - \omega_p$ , where our control frequency is  $\delta_{kq} = (\bar{\omega}_k - \Omega_q)/2$  for a fixed pump frequency (in using external-internal resonance pump frequency of  $\omega_p = \omega_{k-q}$ ). For the photon-phonon coupling we use  $f = 3$  MHz (to neglect the dependent on wavenumbers in this region). In figure (4.a) we plot the upper and lower polariton dispersion. The plot represents the polariton frequencies,  $\Omega^\pm$  (relative to the fixed pump frequency  $\omega_p$ ), as a function of the detuning,  $\delta_{kq}$ , where we change  $\bar{\omega}_k$  relative to a fixed  $\Omega_q$ . Around the intersection point, at  $\bar{\omega}_k = \Omega_q$ , the photon and phonon modes are mixed and split to give two polariton modes, with rabi splitting frequency of  $2|f|$ . In figure (4.b) we plot the photon and phonon factors in the formation of polaritons. Namely, we plot  $|X_{kq}^\pm|^2$  and  $|Y_{kq}^\pm|^2$  as a function of  $\delta_{kq}$ . At large negative detuning the lower polariton branch becomes photonic with  $|Y^-|^2 \approx 1$  and  $|X^-|^2 \approx 0$ , and the upper polariton branch becomes phononic with  $|Y^+|^2 \approx 0$  and  $|X^+|^2 \approx 1$ . The opposite for large positive detuning, the lower polariton branch becomes phononic with  $|Y^-|^2 \approx 0$  and  $|X^-|^2 \approx 1$ , and the upper polariton branch becomes photonic with  $|Y^+|^2 \approx 1$  and  $|X^+|^2 \approx 0$ . Around resonance the upper and lower polariton branches are significant mix of photons and phonons. At  $\delta_{kq} \approx 0$  the polaritons are half photonic and half phononic, that is  $|X^\pm|^2 = |Y^\pm|^2 \approx 1/2$ .

The photon and phonon damping rates can be included phenomenologically by the replacement  $\omega_k \rightarrow \omega_k - i\gamma/2$  and  $\Omega_q \rightarrow \Omega_q - i\Gamma/2$ , where  $\gamma$  is the photon damping rate, and  $\Gamma$  is the phonon damping rate. This replacement leads to the complex polariton frequencies  $\bar{\Omega}_{kq}^\pm$ , which can be approximated in the strong coupling regime by  $\bar{\Omega}_{kq}^\pm = \Omega_{kq}^\pm - i\Gamma_{kq}^\pm$ , with the effective polariton damping rate

$$\Gamma_{kq}^\pm = |X_{kq}^\pm|^2 \frac{\Gamma}{2} + |Y_{kq}^\pm|^2 \frac{\gamma}{2}. \quad (18)$$

#### A. BIO in Linear Nanoscale Waveguides

We present here the input-output formalism in the frame of the polariton picture. For the linear waveguide, that is represented in figure (2), the electromagnetic fields at the left and right sides of the waveguide are given by

$$H_R = \sum_k \int d\omega'_k \hbar\omega'_k c_R^\dagger(\omega'_k) c_R(\omega'_k),$$

$$H_L = \sum_k \int d\omega'_k \hbar\omega'_k c_L^\dagger(\omega'_k) c_L(\omega'_k), \quad (19)$$

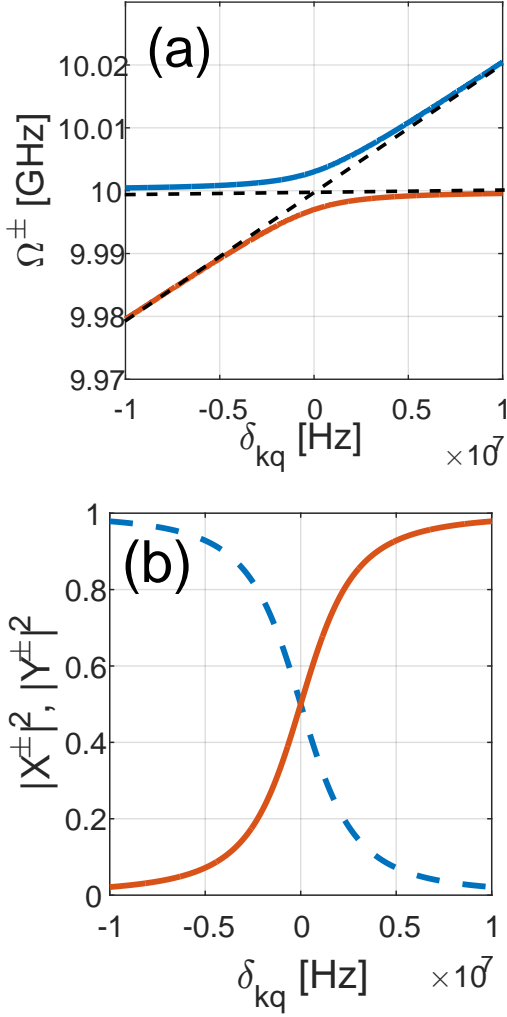


FIG. 4: (a) The upper and lower polariton frequencies,  $\Omega^\pm$ , as a function of the detuning  $\delta_{kq}$ . The horizontal dashed line is for the fixed acoustic phonon, and the linear dashed line is of the photon mode. (b) The photon and phonon fractions  $|X_{kq}^\pm|^2$  and  $|Y_{kq}^\pm|^2$  as a function of  $\delta_{kq}$ . For the lower polariton branch, the dashed line is the photonic fraction and the solid line for the phononic fraction, and the opposite for the upper polariton branch.

with the interaction Hamiltonians

$$\begin{aligned}
 V_R &= \sum_k \int d\omega'_k i\hbar u_R(\omega'_k) \left( c_R^\dagger(\omega'_k) a_k - a_k^\dagger c_R(\omega'_k) \right), \\
 V_L &= \sum_k \int d\omega'_k i\hbar u_L(\omega'_k) \left( c_L^\dagger(\omega'_k) a_k - a_k^\dagger c_L(\omega'_k) \right),
 \end{aligned} \tag{20}$$

where the coupling parameters are  $u_R(\omega'_k)$  and  $u_L(\omega'_k)$ . Using the inverse transformation of (13), the photon operator can be written in term of the polariton operators by

$$a_k = \sum_\mu Y_{kq}^{\mu*} A_{kq}^\mu. \tag{21}$$

The equations of motion for the polariton operators, considering coupling at the left and right mirrors, are

$$\begin{aligned}
 \frac{d}{dt} A_{kq}^\mu &= -i\bar{\Omega}_{kq}^\mu A_{kq}^\mu + \sqrt{u} Y_{kq}^\mu c_k^{in} - u Y_{kq}^\mu a_k, \\
 \frac{d}{dt} A_{kq}^\mu &= -i\bar{\Omega}_{kq}^\mu A_{kq}^\mu - \sqrt{u} Y_{kq}^\mu c_k^{out} + u Y_{kq}^\mu a_k,
 \end{aligned} \tag{22}$$

where  $c_k^{in} = c_{Lk}^{in} + c_{Rk}^{in}$ , and  $c_k^{out} = c_{Lk}^{out} + c_{Rk}^{out}$ . We assumed two identical mirrors with coupling parameter  $u$ . We have the boundary conditions

$$\sqrt{u} a_k = c_{Lk}^{in} + c_{Lk}^{out}, \quad \sqrt{u} a_k = c_{Rk}^{in} + c_{Rk}^{out}. \tag{23}$$

The incident probe field is taken only from the left side, then  $c_k^{in} = c_{Lk}^{in}$ , and  $c_{Rk}^{in} = 0$ .

Taking Fourier transform of the equations into  $\omega$ -space, we get the equations

$$\begin{aligned}
 i(\bar{\Omega}_{kq}^\mu - \omega) \tilde{A}_{kq}^\mu &= \sqrt{u} Y_{kq}^\mu \tilde{c}_{Lk}^{in} - u Y_{kq}^\mu \tilde{a}_k, \\
 i(\bar{\Omega}_{kq}^\mu - \omega) \tilde{A}_{kq}^\mu &= -\sqrt{u} Y_{kq}^\mu (\tilde{c}_{Lk}^{out} + \tilde{c}_{Rk}^{out}) + u Y_{kq}^\mu \tilde{a}_k.
 \end{aligned} \tag{24}$$

The first equation, using (21), yields

$$\tilde{a}_k = -i \frac{\sqrt{u} \Lambda_{kq}}{1 - iu\Lambda_{kq}} \tilde{c}_{Lk}^{in}, \tag{25}$$

where

$$\Lambda_{kq} = \sum_\mu \frac{|Y_{kq}^\mu|^2}{\bar{\Omega}_{kq}^\mu - \omega}. \tag{26}$$

Using the boundary conditions

$$\sqrt{u} \tilde{a}_k = \tilde{c}_{Lk}^{in} + \tilde{c}_{Lk}^{out}, \quad \sqrt{u} \tilde{a}_k = \tilde{c}_{Rk}^{out}, \tag{27}$$

we get the reflection complex amplitude

$$r = |r| e^{i\phi_r} = \frac{\tilde{c}_{Lk}^{out}}{\tilde{c}_{Lk}^{in}} = \frac{-1}{1 - iu\Lambda_{kq}}, \tag{28}$$

and the transmission complex amplitude

$$t = |t| e^{i\phi_t} = \frac{\tilde{c}_{Rk}^{out}}{\tilde{c}_{Lk}^{in}} = -i \frac{u\Lambda_{kq}}{1 - iu\Lambda_{kq}}. \tag{29}$$

The reflection parameter is

$$R = \frac{\langle \tilde{c}_{Lk}^{out\dagger} \tilde{c}_{Lk}^{out} \rangle}{\langle \tilde{c}_{Lk}^{in\dagger} \tilde{c}_{Lk}^{in} \rangle} = \frac{1}{|1 - iu\Lambda_{kq}|^2}, \tag{30}$$

and the transmission parameter is

$$T = \frac{\langle \tilde{c}_{Rk}^{out\dagger} \tilde{c}_{Rk}^{out} \rangle}{\langle \tilde{c}_{Lk}^{in\dagger} \tilde{c}_{Lk}^{in} \rangle} = \frac{u^2 |\Lambda_{kq}|^2}{|1 - iu\Lambda_{kq}|^2}, \tag{31}$$

using  $T + R + A = 1$  gives the absorption parameter

$$A = \frac{iu(\Lambda_{kq}^* - \Lambda_{kq})}{|1 - iu\Lambda_{kq}|^2}. \tag{32}$$

We illustrate the results using typical numbers for nanoscale waveguides. The photon damping rate is  $\gamma = 10^5$  Hz, the phonon damping rate is  $\Gamma = 10^6$  Hz, the mirror coupling is  $u = 10^6$  Hz, and the photon-phonon coupling is  $g = 10^4$  Hz. The signal photon mode at wavenumber  $k$  is taken to be  $\omega_k = 10^{14}$  Hz, the phonon mode at  $q$  is  $\Omega_q = 10^{10}$  Hz, and the pump photon mode at wavenumber  $k - q$  is taken to be  $\omega_{k-q} = \omega_k - \Omega_q$ .

We present first the case of small pump intensity of  $n_{k-q}^{in} = 10^8$  Hz, and for resonance external-internal pump, that is  $\omega_p = \omega_{k-q}$ . We present the signal transmission spectrum in figure (5.a), and the signal reflection spectrum in figure (5.b), as a function of the detuning frequency ( $\omega - \omega_k$ ). We are in the weak coupling regime, hence one peak appears in the transmission, and one dip in the reflection, at the signal field frequency, that is at  $\omega = \omega_k$ . The concept of polaritons is irrelevant here, where full transmission and small reflection appear around resonance.

Next we increase the pump intensity in order to achieve the strong coupling regime keeping the case of external-internal resonance at  $\omega_p = \omega_{k-q}$ . We use the pump intensity around  $n_{k-q}^{in} = 10^{11}$  Hz. We plot the signal transmission  $T$  in figure (6.a), and its phase shift in figure (6.b), as a function of the frequency  $\omega - \omega_q$ , for the case of resonance pump, that is  $\omega_p = \omega_{k-q}$ . No transmission appears now around resonance. We plot the signal reflection  $R$  in figure (7.a), and its phase shift in figure (7.b), as a function of the frequency  $\omega - \omega_q$ . Here, complete reflection appears around resonance and we get BIO.

The opacity appears as the photons and phonons coherently are mixed and split to give two polariton modes that are separated at the intersection point by a frequency splitting of twice the coupling parameter (Rabi frequency). Without the pump field, the external probe field of frequency  $\omega_s$  has a resonance with a waveguide mode at  $\omega_k$ . The pump field removes this resonance through SBS, and new two resonances appear at the polariton frequencies. We conclude that the real excitations in the strong coupling regime are polaritons and not independent photons and phonons.

## B. BIT in Ring Nanoscale Waveguides

We consider the case of a one dimensional nanoscale waveguide that forms a ring, which is represented in figure (3). The treatment of the previous section holds here, as we used periodic boundary conditions for the propagating light inside the linear waveguide. Now we remove the edge mirrors and connect the two sides to form a ring. The input-output coupling is achieved by an external optical nanofiber that coupled to the waveguide ring at a fixed point.

In terms of polaritons we get the same system of equations as in eqs.(24), where the input and output fields

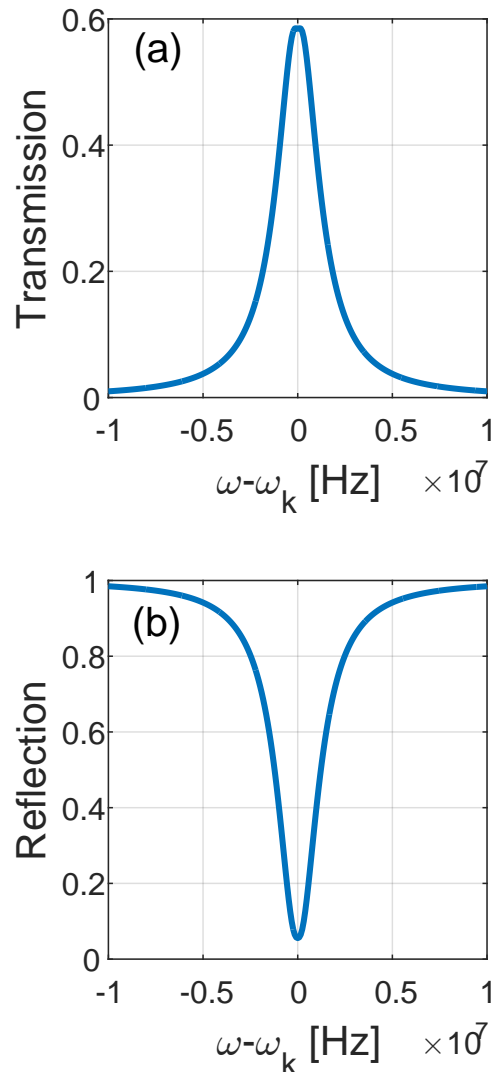


FIG. 5: Linear waveguide. (a) The signal transmission  $T$  vs. frequency  $\omega - \omega_k$ . (b) The signal reflection  $R$  vs. frequency  $\omega - \omega_k$ . The pump is at resonance,  $\omega_p = \omega_{k-q}$ , at low intensity of  $n_{k-q}^{in} = 10^8$  Hz.

obey now the boundary condition

$$\sqrt{u} a_k = c_k^{in} + c_k^{out}. \quad (33)$$

Repeating the calculations for a ring waveguide, we get the complex amplitude

$$t = |t| e^{i\phi_r} = \frac{\tilde{c}_k^{out}}{\tilde{c}_k^{in}} = \frac{-1}{1 - iu\Lambda_{kq}}, \quad (34)$$

with the transmission parameter

$$T = \frac{\langle \tilde{c}_k^{out\dagger} \tilde{c}_k^{out} \rangle}{\langle \tilde{c}_k^{in\dagger} \tilde{c}_k^{in} \rangle} = \frac{1}{|1 - iu\Lambda_{kq}|^2}, \quad (35)$$

and using  $T + A = 1$  in order to get the absorption parameter. The present  $t$  is identical to  $r$  in the previous

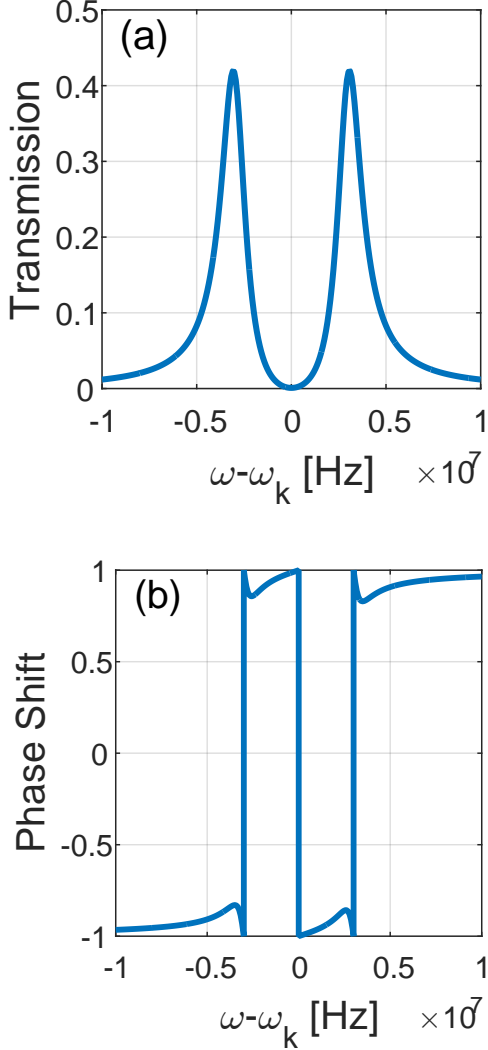


FIG. 6: Linear waveguide. (a) The signal transmission  $T$  vs. frequency  $\omega - \omega_k$ . (b) The signal transmission phase shift  $\phi_t$  vs. frequency  $\omega - \omega_k$ . The pump is at resonance,  $\omega_p = \omega_{k-q}$ , of large intensity  $n_{k-q}^{in} = 10^{11}$  Hz.

case of a linear waveguide, where all the above plots of  $r$ , in figure (7), are the same for the present  $t$ . Hence for a ring waveguide we get BIT for the light propagating in the external fiber, rather than BIO in the above case of linear waveguides. Namely, in the absence of the pump field the probe field is strongly coupled to the waveguide signal field and only small part transmitted along the fiber. But once the pump is switched on the fiber-waveguide resonance at the probe frequency blocked and the probe light continue along the fiber without entering the waveguide. Namely the system becomes transparent for the probe field.

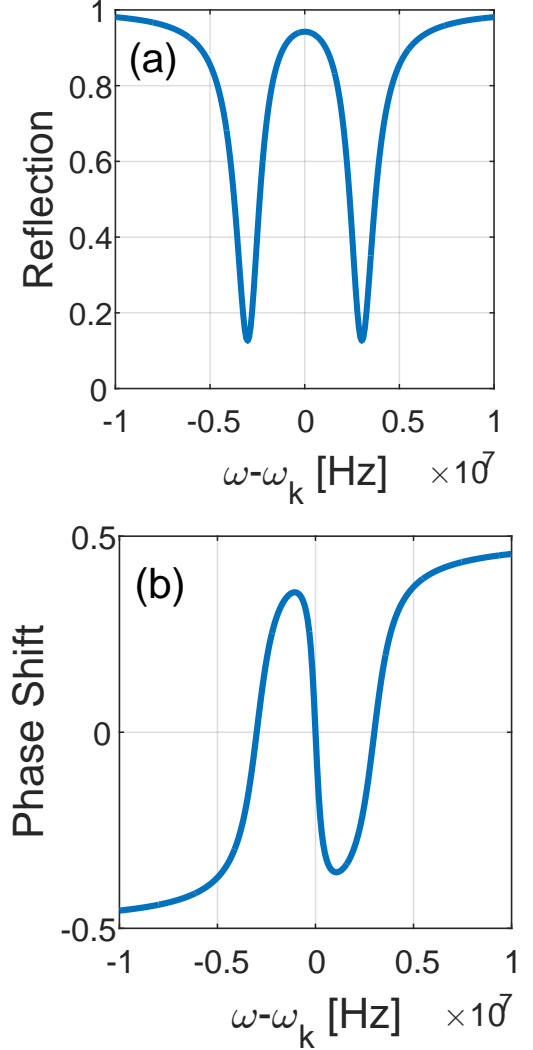


FIG. 7: Linear waveguide. (a) The signal reflection  $R$  vs. frequency  $\omega - \omega_k$ . (b) The signal reflection phase shift  $\phi_t$  vs. frequency  $\omega - \omega_k$ . The pump is at resonance,  $\omega_p = \omega_{k-q}$ , of large intensity  $n_{k-q}^{in} = 10^{11}$  Hz. For a ring waveguide the plots represent the transmission and its phase shift of the signal field through the external nanofiber.

#### IV. CONCLUSIONS

We adopt the concept of phonon-polariton in order to explain the phenomena of BIO in linear waveguides and BIT in ring waveguides. We show how the strong coupling regime among a phonon and a photon can be achieved through SBS in the presence of a strong pump field. Coherent oscillations between the phonon and photon fields inside a waveguide is possible once the effective phonon-photon coupling becomes larger than their damping rates. This regime is reachable for nanoscale waveguides, in which radiation pressure dominates over conventional electrostriction, and for long lived phonons within the waveguide.

The input-output method provides us with a tool for observing the system collective eigenmodes, by coupling the internal waveguide states to the external radiation field through the effective mirrors in linear waveguides and through a nearby nanofiber in ring waveguides. The method yields linear optical spectra and phase shifts for an external probe field, where the intensity of the pump field serves us as a control parameter. In a linear waveguide at low pump intensity a single peak appears in the transmission spectrum and a single dip in the reflection spectrum. But for high pump intensity, once the strong coupling regime is achieved, two peaks appear in the transmission spectrum and two dips in the reflection spectrum, which are a signature for the formation of phonon-polaritons. Namely, at a frequency where a transparency is expected in a linear waveguide an opacity obtained due to SBS. Similar consideration hold for a ring waveguide, but in the strong coupling where an

opacity is expected a transparency is obtained.

The advantage of nanoscale waveguides is in their easy integration into all-optical on-chip platform. BIT and BIO introduced in the present paper can be of importance for quantum information processing and communication involving photons and phonons. BIT and BIO can be tailored for realizing phonon and photon Brillouin laser. Phonon-polaritons, as exotic states made of a coherent mix of light and mechanical excitations, are a promising candidate for the implementation of non-classical and entangled states.

### Acknowledgment

The author thanks Klemens Hammerer for very fruitful discussions.

- 
- [1] R. W. Boyd, *Nonlinear Optics* (Elsevier, Amsterdam, 2008), 3rd ed.
  - [2] G. P. Agrawal, *Nonlinear Fiber Optics* (Elsevier, Amsterdam, 2013), 5th ed.
  - [3] R. Y. Chiao, C. H. Townes, and B. P. Stoicheff, *Phys. Rev. Lett.* **12**, 592 (1964).
  - [4] P. T. Rakich, C. Reinke, R. Camacho, P. Davids, and Z. Wang, *Phys. Rev. X* **2**, 011008 (2012).
  - [5] R. Van Laer, B. Kuyken, D. Van Thourhout, and R. Baets, *Nature Photonics* **9**, 199 (2015).
  - [6] H. Zoubi and K. Hammerer, *Phys. Rev. A* **94**, 053827 (2016).
  - [7] L. Thevenaz, *Nature Photonics* **2**, 474 (2008).
  - [8] G. Bahl, M. Tomes, F. Marquardt, and T. Carmon, *Nature Physics* **8**, 203 (2012).
  - [9] G. S. Agarwal and S. S. Jha, *Phys. Rev. A* **88**, 013815 (2013).
  - [10] J.-C. Beugnot, S. Lebrun, G. Pauliat, H. Maillotte, V. Laude, and T. Sylvestre, *Nature Communications* **5**, 5242 (2014).
  - [11] M. Merklein, B. Stiller, K. Vu, S. J. Madden, and B. J. Eggleton, *nature Communications* **8**, 574 (2017).
  - [12] H. Zoubi and K. Hammerer, *Physical Review Letters* **119**, 123602 (2017).
  - [13] B. J. Eggleton, C. G. Poulton, and R. Pant, *Adv. Opt. Photon.* **5**, 536 (2013).
  - [14] R. Pant, C. G. Poulton, D.-Y. Choi, H. Mcfarlane, S. Hile, E. Li, L. Thevenaz, B. Luther-Davies, S. J. Madden, and B. J. Eggleton, *Opt. Express* **19**, 8285 (2011).
  - [15] H. Shin, W. Qiu, R. Jarecki, J. A. Cox, R. H. Olsson III, A. Starbuck, Z. Wang, and P. T. Rakich, *Nature Communications* **4**, 1944 (2013).
  - [16] R. V. Laer, A. Bazin, B. Kuyken, R. Baets, and D. V. Thourhout, *New Journal of Physics* **17**, 115005 (2015).
  - [17] E. A. Kittlaus, H. Shin, and P. T. Rakich, *Nature Photonics* **10**, 463 (2015).
  - [18] M. Fleischhauer, A. Imamoglu, and J. P. Marangos, *Rev. Mod. Phys.* **77**, 633 (2005).
  - [19] A. H. Safavi-Naeini, T. P. M. Alegre, J. Chan, M. Eichenfield, M. Winger, Q. Lin, J. T. Hill, D. E. Chang, and O. Painter, *Nature* **472**, 69 (2011).
  - [20] S. Weis, R. Rivière, S. Deléglise, E. Gavartin, O. Arcizet, A. Schliesser, and T. J. Kippenberg, *Science* **330**, 1520 (2010).
  - [21] J. Kim, M. C. Kuzyk, K. Han, H. Wang, and G. Bahl, *Nature Physics* **11**, 275 (2015).
  - [22] M. Aspelmeyer, T. J. Kippenberg, and F. Marquardt, *Rev. Mod. Phys.* **86**, 1391 (2014).
  - [23] C. W. Gardiner and P. Zoller, *Quantum Noise* (Springer-Verlag, Berlin, 2010).
  - [24] D. F. Walls and G. J. Milburn, *Quantum Optics* (Springer-Verlag, Berlin, 2008).
  - [25] E. Vetsch, D. Reitz, G. Sague, R. Schmidt, S. T. Dawkins, and A. Rauschenbeutel, *Phys. Rev. Lett.* **104**, 203603 (2010).
  - [26] A. Goban, K. S. Choi, D. J. Alton, D. Ding, C. Lacroute, M. Pototschnig, T. Thiele, N. P. Stern, and H. J. Kimble, *Phys. Rev. Lett.* **109**, 033603 (2012).
  - [27] E. Taillaert, D. Van-Laere, G. Ayre, R. Bogaerts, S. T. Van-Thourhout, R. Bienstman, and A. Baets, *Jpn. J. Appl. Phys.* **45**, 6071 (2006).